

A mathematical model for flight guidance in honeybee swarms

R. C. Fetecau * A. Guo *

July 30, 2012

Abstract

When a colony of honeybees relocates to a new nest site, less than 5% of the bees (the scout bees) know the location of the new nest. Nevertheless, the small minority of informed bees manages to provide guidance to the rest and the entire swarm is able to fly to the new nest intact. The stalker bee hypothesis, one of the several theories proposed to explain the guidance mechanism in bee swarms, seems to be supported by recent experimental observations. The theory suggests that the informed bees make high-speed flights through the swarm in the direction of the new nest, hence conspicuously pointing to the desired direction of travel. This work presents a mathematical model of flight guidance in bee swarms based on the stalker bee hypothesis. Numerical experiments, parameter studies and comparison with experimental data are presented.

1 Introduction

Organized and directional movement of large groups of individuals is very common in many animal species. Fish swim in schools and birds fly in flocks for the purpose of enhancing the foraging success [1, 2], reducing the risk of predation [3], and possibly for increasing the hydrodynamic efficiency [4]. Coordinated movement in a group can be achieved when each individual reacts to its neighbour movements (allelomimetic behaviour), while at the same time maintains a certain, relatively constant, distance from its immediate neighbours [5]. In this paper we are concerned with the flight of a honeybee swarm toward a new nest site. The intriguing feature of this directed and organized flight is that at the time of liftoff, less than 5% of the bees (the “scout bees”) have visited the new nest site and therefore have information about its location [6]. Nevertheless, the scout bees manage to transfer directional information and steer the swarm to the new home. This coordinated flight of a honeybee swarm contrasts sharply with most migration movements in fish or birds, where most (if not all) individuals have information about the destination, provided by either their innate homing ability [7] or learned behaviour [8].

Honeybee swarms are produced by colony fissioning, when the mother queen and about two thirds of the worker bees leave the parental nest to establish a new colony (reviewed in [9]). Upon leaving the nest, the swarm first settles into a beard-like cluster on a nearby tree branch. Soon after, hundreds of scout bees fly out in search of potential new nest sites. Once a scout bee identifies a suitable nest, it returns to the cluster and performs a waggle dance to advertise it (the waggle dance encodes information about the location, as well as the desirability of the potential nest) [10].

*Department of Mathematics, Simon Fraser University, 8888 University Dr., Burnaby, BC V5A 1S6, Canada, email: {van,yga24}@sfu.ca

This process is iterated several times, with scout bees inspecting the vigorously advertised locations and returning to cast their own assessment. A quorum is typically reached, followed by the take off of the entire swarm and its flight to the chosen site. All these stages in the relocation of a honeybee swarm to a new nest have been recently reviewed in the excellent book by T. Seeley [11].

It is important to note that the large majority of the bees (more than 95%) do not scout and simply remain quiescent through the search and the decision-making process. They do not know the location of the new nest at the time of lift-off and rely on the scout bees to guide them. Various theories have been formulated regarding the mechanisms of flight guidance in honeybee swarms. An early theory [12] hypothesized that the guidance is chemical in nature, with uninformed bees navigating according to the pheromone cues emitted by the scout bees. This plausible hypothesis has been falsified by Beekman *et al.* [13]: a swarm of bees with pheromone glands shut was equally capable of flying to the new nest.

Two other hypotheses, called here the “subtle guide” and the “streaker bee” hypothesis, have stood the time test. Both hypotheses start from the premise that the guidance is visual, but they differ essentially on how the scout bees provide guidance information to the rest of the swarm. The subtle guide hypothesis assumes that there is no conspicuous signalling mechanism originating from the scout bees, and that the steering of the swarm is achieved just by their tendency to fly in the direction of the new nest. This hypothesis was successfully tested with a mathematical model by Couzin *et al.* [14]. An interesting aspect of their model is that for a specified accuracy (quality of information transfer), the larger is the group, the smaller is the proportion of informed individuals needed to achieve the given accuracy. As a result, large groups need only a small percentage of informed individuals to achieve maximal guiding accuracy.

The streaker bee hypothesis, originally proposed by Lindauer [10], suggests that the informed bees make high-speed flights through the swarm in the direction of the new nest, hence conspicuously pointing to the desired direction of travel. Once they reach the front of the swarm, they return at low speeds to the back, by flying along the edges of the swarm. The key differences between the streaker bee and the subtle guide hypotheses lie in whether or not the naive individuals favour alignment with fast-flying bees and whether or not the scout bees streak (hence the name “streaker bees”) through the swarm. The streaker bee hypothesis has been tested with both experimental observations [13, 6, 15] and mathematical models [16, 17], some of which we summarize below.

Beekman *et al.* [13] took photos of airborne swarms and showed that a small minority of the bees do streak through it at the maximum flight speed of a worker bee, while the rest of the bees fly about within the swarm in slow and looping flights. Also, photographic analysis indicated that the streaker bees prefer to streak in the upper half of the bee cloud, where they can be more easily seen by the other bees. Schultz *et al.* [15] performed a video analysis of a flying swarm using computer tracking algorithms and computed the individual trajectories of bees in the swarm. They measured each bee’s position, flight direction and speed. The study confirmed the streaker bee hypothesis and the fact that the speedsters tend to locate themselves in the top portion of the swarm. Another field experiment [18] considered a migrating bee swarm exposed to conflicting directional information coming from fast-moving foraging bees flying in a direction perpendicular to the swarm’s intended flight path. The heavy traffic of fast-flying foragers disrupted the flight of the swarm, hence supporting the streaker bee hypothesis.

Janson *et al.* [16] developed a mathematical model to test the streaker bee hypothesis. The time-discrete model considers three interactions rules among individuals (cohere, align and avoid), as well as a random movement. The velocity of each individual is updated according to a weighted

sum of these movement rules. The model has been revisited by Diwold *et al.* [17] who use a topological neighbourhood metric [19], and restrict the alignment interaction to act only with respect to neighbours that are at least twice as fast as the reference individual. The model incorporates the streaker bee hypothesis, that is, informed bees streak through the swarm and fly back (with lower speeds) once they reach the front. The results show that the model can mimic various qualitative and quantitative behaviours of real swarms, including some anomalous behaviours such as splitting.

In the present research we take a different approach and model the swarm flight with a system of ordinary differential equations (ODE's). The use of ODE's to study group behaviour has resulted in an impressive collection of complex emerging patterns (clumps, rings, annular states, single and double milling solutions, etc) [20, 21, 22, 23]. Applications of such models are very diverse, ranging from biological swarms [24] to self-assembly of nano-particles [25] and coordinated control of unmanned vehicles [26]. Typically, the motion of individuals in ODE models is governed by Newton's second law of motion, where the force incorporates social interactions and self-propulsion. We consider such a model in this work, with the additional feature of having informed and uninformed individuals, the former performing streaks through the swarm.

We present two mathematical models based on the streaker bee hypothesis. The two models differ in the assumptions made on the flight of the streakers. In one model, streakers accelerate through the swarm with constant acceleration, while in the other, streakers fly at constant velocities. We present evidence that the first model is more efficient in terms of flight guidance. Follower bees evolve according to Newton's second law, with force fields designed to capture social interactions among individuals. Attraction and repulsion are modelled via a pairwise interaction potential, with exponentially decaying interactions [20, 21]. Alignment is modelled through an alignment force, as in the Cucker-Smale model for flocking [27]. An important caveat is that we also consider a cone of vision/ blind zone of the flying bees, a feature which is essential in the flight of a real bee swarm. Various numerical results are presented to address the qualitative behaviour of the model in terms of swarm speed and efficiency, flight angle distribution, trajectory of centre of mass, etc. We discuss the advantages of returning faster/slower to the rear, as well as the flight efficiency as the number of streaker bees decreases. Finally, a discussion section relates the findings using this model with data from experiments.

2 The mathematical model

Consider a swarm of N individuals with N_f follower (uninformed) bees and N_s streaker (leader) bees. In all simulations we take $\frac{N_s}{N} < 0.05$ to model realistic percentage of streakers in actual swarms (less than 5%). An individual bee i has position \mathbf{x}_i and velocity \mathbf{v}_i , which evolve continuously in time, according to a system of ordinary differential equations. Followers and streaker bees have separate equations of motion.

In setting up the mathematical model, we assume that all bees (both followers and streakers) interact via a pairwise attractive-repulsive potential that describe the tendency of the bees to cohere to the swarm, as well as to avoid collisions with the neighbours. In addition, the follower bees experience a force that tends to align their velocities with faster-flying neighbours. In contrast, streaker bees do not align with neighbours, but simply fly in the desired direction of motion. Once they reach the front, they return to the back of the swarm. We consider two models for the flight of the streaker bees: i) a model in which the streaker bees accelerate as they move from the rear of the swarm to its front, and ii) a model where the streaker bees fly at constant (high) speeds

through the swarm. The recent video processing study from [15] seems to favour the first scenario. Finally, we introduce a cone of vision/ blind zone in order to account for realistic limitations of a bee's vision, as well as to treat appropriately the return of a streaker bee, which occurs in less visible parts of the bee cloud.

Equations of motion for followers. The motion of the follower (uninformed) bees is modelled by the following set of equations ($i = 1, \dots, N_f$):

$$\frac{d\mathbf{x}_i}{dt} = \mathbf{v}_i \quad (1a)$$

$$\frac{d\mathbf{v}_i}{dt} = -\nabla U_i + \mathbf{F}_i, \quad (1b)$$

where U_i is an attractive-repulsive potential and \mathbf{F}_i is an alignment force acting on the i^{th} follower bee.

The potential U_i describes the attraction and repulsion interactions among bees. We consider here the Morse potential, weighted by blind zone coefficients:

$$U_i = \sum_{j \neq i} w_{ij} \left(-C_a e^{-\frac{|\mathbf{x}_i - \mathbf{x}_j|}{l_a}} + C_r e^{-\frac{|\mathbf{x}_i - \mathbf{x}_j|}{l_r}} \right). \quad (2)$$

Here, C_a and C_r are the attraction and repulsion strengths, respectively, l_a and l_r are the attraction and repulsion ranges, respectively, and the coefficients w_{ij} are weights representing the blind zone component of bee j with respect to bee i . By taking the product with the weights w_{ij} , we account for only the bees j that are within bee i 's cone of vision. We describe the blind zone in detail later in this section (see equation (7)). The Morse potential is an appropriate choice for a zonal model of collective motion, as it delineates zones of repulsion (close to the individual) and attraction (at larger distances), and as such, it was used in several other ODE aggregation models [20, 21, 24]. Typically, $C_r > C_a$ and $l_a > l_r$ because swarms have strong short-distance repulsion and weaker long-distance attraction. Figure 1(a) shows plots of the Morse function for various values of the parameters. Positive values (above the horizontal dashed line) correspond to repulsion, while negative values to attraction. The dash-dotted plot corresponds to shorter repulsion and attraction ranges (smaller l_r and l_a), as compared to the solid line one. Note that interactions decay exponentially with distance.

Alignment forces have been considered previously in the context of models for flocking (for instance, the Cucker-Smale model [27]). Individuals tend to align their velocities with those of their neighbours, and the extent to which alignment occurs should depend on the relative distance between two interacting individuals, their locations in each other's cone of vision, and also, very pertinent to the bee flight considered here, the amount by which the speeds of the two individuals differ from each other.

Mathematically, we model the alignment force \mathbf{F}_i by:

$$\mathbf{F}_i = -\frac{C_{al}}{n_i} \sum_{j \neq i} a_{ij} e^{-\frac{|\mathbf{x}_i - \mathbf{x}_j|}{l_{al}}} (\mathbf{v}_i - \mathbf{v}_j), \quad (3)$$

where C_{al} and l_{al} are the alignment strength and range, respectively, n_i is the number of bees that affect bee i 's alignment, and a_{ij} are weights that take the blind zone into account, as well as compare the velocity of the current bee i to that of bee j . If the speed of bee j is greater (in

an amount to be specified by the model) than the speed of the current bee, an alignment force is assigned, otherwise j is considered to have no affect on the current bee as far as alignment is concerned. This modelling hypothesis means that an individual tends to align with fast flying individuals only, and in a swarm, these individuals are typically the streaker bees.

The matrix a_{ij} contains information on how much bee i should align with bee j . We model a_{ij} with the following function

$$a_{ij} = \begin{cases} w_{ij}h \tanh\left(s\left(\frac{|\mathbf{v}_j|}{|\mathbf{v}_i|} - 2\right)\right) & \text{for } \frac{|\mathbf{v}_j|}{|\mathbf{v}_i|} > 2 \\ 0 & \text{for } \frac{|\mathbf{v}_j|}{|\mathbf{v}_i|} \leq 2 \end{cases}, \quad (4)$$

where w_{ij} are the blind zone weights (to be defined in equation (7)), s is a stretch parameter and h is the height of the function \tanh . Note the threshold 2 considered by the model, which means that a follower bee aligns only with individuals which fly at least two times faster than her. A generic plot of a_{ij} (for $w_{ij} = 1$) is shown in Figure 1(b). The current bee i has no alignment interaction with bee j , that is $a_{ij} = 0$, if $|\mathbf{v}_j| < 2|\mathbf{v}_i|$. There is a relatively sharp increase when $|\mathbf{v}_j| > 2|\mathbf{v}_i|$ with steepness controlled by s , followed by a levelling off at value h . By taking the product of the \tanh function with w_{ij} we weight the alignment interactions according to the blind zone.

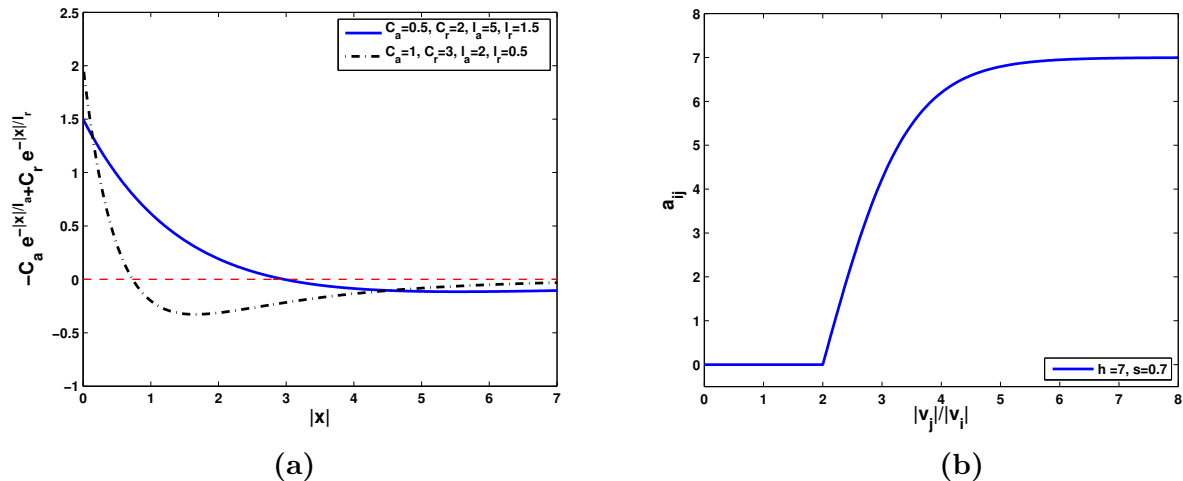


Figure 1: (a) Plot of the Morse potential used in equation (2). Positive values (above the dashed line) correspond to short range repulsion, and negative values represent long range attraction. (b) Plot of function a_{ij} from (4) for $w_{ij} = 1$. The values are zero when $|\mathbf{v}_j| \leq 2|\mathbf{v}_i|$, increase relatively steeply as $|\mathbf{v}_j| > 2|\mathbf{v}_i|$, and they asymptote at $h = 7$. Follower bees align only with individuals which fly at least two times faster than them.

Remark. An interesting question is what happens if the uninformed bees are attracted to (instead of aligning with) the streaker bees. To test the outcome of such a modelling assumption, we used a \tanh function as in (4) to introduce a *dynamic* attraction coefficient C_a for follower bees, which makes them more attracted to faster flying individuals. We either removed the alignment completely or considered both alignment and preferential attraction. We did not find however that this enhanced attraction helps the steering of the swarm in our models. It is very possible that

other ways of implementing this feature would result in a more efficient steering, and we plan to address this issue in future work.

Equations of motion for streakers. The streaker bees fly at high speeds toward the desired location, reach the swarm’s front, then return to the rear and start over. Their movement is not governed by an alignment force, as they know in which direction to fly. Also, their interaction with the rest of the bees (due to attraction and repulsion) is limited, as the streakers’ main role is to guide the swarm to the new nest. Therefore, we ignore pairwise interactions and alignment forces and consider two very simple models for the flight of the streakers ($i = 1, \dots, N_s$):

1. Model I: Streaker bees accelerate through the swarm with constant acceleration:

$$\frac{d\mathbf{x}_i}{dt} = \mathbf{v}_i \tag{5a}$$

$$\frac{d\mathbf{v}_i}{dt} = \mathbf{a}_0. \tag{5b}$$

Here, the vector \mathbf{a}_0 is the (constant) acceleration of the streaker bee. The acceleration vector points in the desired direction of motion when the bee streaks forward and in the opposite direction when the bee returns to the back of the swarm. We also consider different magnitudes for the streaking/ returning acceleration vector.

2. Model II: Streaker bees fly through the swarm with constant speed:

$$\frac{d\mathbf{x}_i}{dt} = \mathbf{v}_0 \tag{6a}$$

$$\frac{d\mathbf{v}_i}{dt} = \mathbf{0}. \tag{6b}$$

The constant speed \mathbf{v}_0 points either in the direction of the target (bees streaking forward) or in the opposite direction (bees returning to the rear). We consider different magnitudes for the two directions of motion, with higher speed when leader bees are streaking forward.

Recent studies using video data processing [15] seem to validate the first model. However the streakers’ flight has not been fully elucidated and other theories (such as Model II) are also possible. In fact, the mathematical model considered by Diwold et al. [17] uses different constant speeds for streaking and returning bees.

Blind zone. Bees have a field of vision [28], which has to be considered in the model, for both follower and leader bees. Optical experiments designed to simulate the visual input of a bee consider the bee’s field of view in their setup [29]. Here we model the field of view mathematically. We describe and illustrate a two-dimensional cone of vision, that is, for individuals which move in a plane. The model presented in the previous paragraphs works in three-dimensions as well, and in that case the cone of vision has to incorporate the extra dimension. For simplicity, we test our model in two dimensions (see numerical results in Section 3) and we present here the cone of vision associated to motion in a plane.

Suppose bee i is a reference bee which has a vision range (denoted below by l_v) and a cone of vision — see Figure 2. Within the cone of vision of bee i we distinguish between a zone of direct

vision (represented by the dark grey area) and a zone of peripheral vision (the light grey area). To model the blind zone weights w_{ij} we start from the following considerations. A bee which is in the direct vision (bee j) should get assigned a higher weight than a bee which lies in the peripheral vision (bee k), while a bee which lies outside of bee i 's vision completely (bee h) should get zero weight. The relative distance between individuals should also play a role, so a distance factor must be considered.

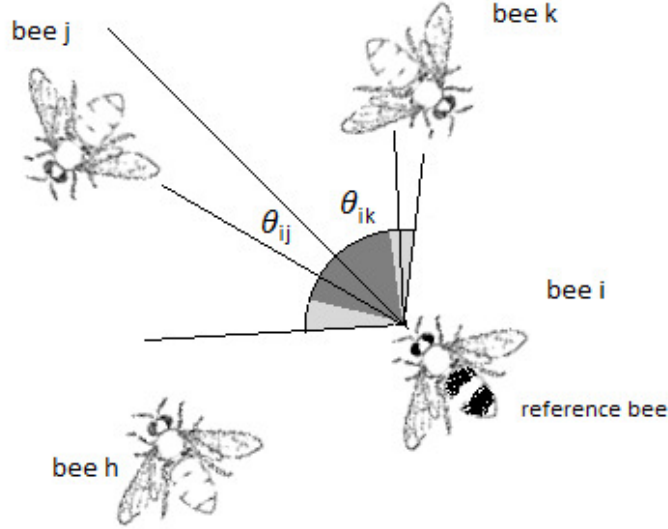


Figure 2: This diagram demonstrates how the blind zone is calculated. Bee i is the reference bee with bees j, k, h in its neighbourhood. The dark grey area is bee i 's direct vision while the light grey area is its peripheral vision. Bee j is within bee i 's direct vision and gets assigned a higher weight than bee k , which lies in bee i 's peripheral vision. Bee h lies outside of bee i 's vision completely and gets assigned zero weight. Hence bee i is most influenced by bee j , followed by bee k , and bee h has no effect on the reference bee.

Consider now the reference bee i located at \mathbf{x}_i , a generic bee j located at \mathbf{x}_j , and denote by θ_{ij} the angle between the relative position $\mathbf{x}_j - \mathbf{x}_i$ and the velocity \mathbf{v}_i of the reference bee — see Figure 2. Following the previous considerations, individuals in front of or close to the reference individual (small θ_{ij} and small $\mathbf{x}_j - \mathbf{x}_i$, respectively) will be given higher weights w_{ij} . The weights w_{ij} used in (2) and (4) that describe the cone of vision/blind zone of bee i are modelled by the following function:

$$w_{ij} = (0.5 \tanh(a(\cos \theta_{ij} + (1 - b/\pi))) + 0.5) e^{-\frac{|\mathbf{x}_i - \mathbf{x}_j|}{l_v}}, \quad (7)$$

which we describe in detail below.

The function $0.5 \tanh(a(\cos \theta + (1 - \frac{b}{\pi}))) + 0.5$ captures mathematically the direct/peripheral vision and blind zone. Figure 3 shows the graph of the function for several values of the parameters

a and b . The function captures the needed features: large and almost constant values in a certain interval around $\theta = 0$ (direct vision), steep decay at the periphery (peripheral vision) and zero values in the blind zone. The parameters a and b control the steepness and width of the cone of vision, respectively.

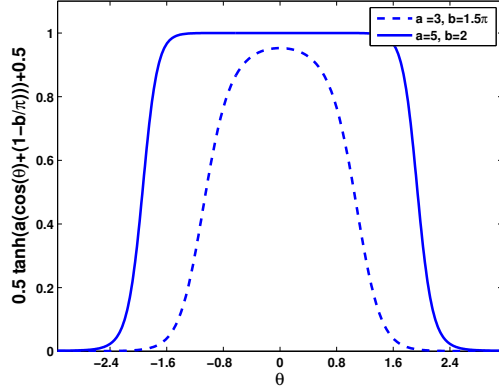


Figure 3: Weighting the cone of vision: plots of the function $0.5 \tanh(a(\cos \theta + (1 - \frac{b}{\pi}))) + 0.5$ from (7) with different a and b (a controls the steepness of the graph and b controls the width). The function takes large and almost constant values in the cone of vision, has steep decay at the periphery and has zero values in the blind zone.

The exponentially decaying term is very easy to explain, as it is similar to the distance factors used in (2) and (3)). The coefficients w_{ij} are weighted according to the relative distance $|\mathbf{x}_i - \mathbf{x}_j|$. The range l_v measures how far a bee can see around itself. It can be taken to be a constant or, alternatively, one could consider a non-uniform range of vision, with high values in front and low values at the periphery of the vision cone. Suppose a bee can see a distance of d directly in front ($\theta = 0$), and as we move into peripheral vision, this distance decreases. This can be modelled by the same tanh function plotted in Figure 3, and in simulations we use

$$l_v = d \frac{0.5 \tanh(a(\cos \theta_{ij} + (1 - \frac{b}{\pi}))) + 0.5}{F}, \quad (8)$$

where d is the maximum distance that a honeybee is able to see, and F is a normalizing factor given by

$$F = 0.5 \tanh(a(1 + (1 - b/\pi))) + 0.5.$$

As a simple example, suppose the reference bee i is at the origin and flying in the direction of $(1,0)$ and there is a bee j right in front at position $(4,0)$ and another bee k at position $(15,0)$ then bee j would have a higher weight than bee k because it is closer to bee i . On the other hand, if bee j was at position $(0,1)$ then it would have a much lower weight because it is in bee i 's peripheral vision.

Other features of the model. In addition to the dynamics of the follower and stalker bees governed, respectively, by (1) and either (5) or (6), we include various features in the model in order to make the swarm flight more realistic.

Random flying and redirecting. According to their location in its cone of vision, each follower bee i associates a weight w_{ij} (given by (7)) to each of the other $N - 1$ bees. We calculate the sum $\sum_{j \neq i} w_{ij}$ of all the weights with respect to bee i , in order to quantify the amount of interaction that bee i has with the rest of the bees. If bee i has a significant number of bees in its cone of vision, then it interacts with them and its dynamics is governed by system (1). On the contrary, if this vision indicator falls below a certain value (in simulations taken to be $1/N$), we assign a random velocity to follower bee i , to allow it to come back into stronger contact with the other bees. Follower bees that have gotten to the edge of the swarm (and have an interaction indicator below the threshold) are assigned a random direction and a random velocity, with the x- and y-components both between -0.5 and 0.5 .

Along the same idea, provided the follower bee i gets lost or confused about where to fly and it slows down, with its speed dropping below a certain value (in the simulations set at 0.5), we assign it a full cone of vision (all $w_{ij} = 1$) to give it time to look around and redirect its direction of motion according to the location of the other bees. This feature was necessary for the model to work effectively, by preventing follower bees from getting lost due to them rarely seeing other bees in their cone of vision when flying at relatively low speeds.

Returning stalker bees. The stalker bee hypothesis says that a leader bee will streak through the swarm from the back to the front at a higher velocity than the follower bees, in order to get other bees to follow it. We implement a returning feature in our model, to prevent the stalker bees from flying out of the swarm.

Consider a generic stalker bee s . Bee s flies through the swarm by accelerating/ flying at constant speed in the direction of the new nest (see dynamics governed by (5)/(6)). Similar to above, we calculate the vision indicator $\sum_{j \neq s} w_{sj}$ corresponding to bee s . Once this indicator drops below a threshold, i.e., the stalker bee has reached the front of the swarm, bee s turns around and flies to the back of the swarm. In simulations of Model I we reset the velocity to 0 and change the orientation and magnitude of \mathbf{a}_0 . In Model II, stalkers bee turn and start flying instantaneously at constant speed in the opposite direction.

In simulations, the thresholds of the vision indicator used for turning are $0.5/N_f$ when the stalker bee reaches the front and $2/N_f$ when the stalker bee reaches the back. This means that a stalker bee would turn sooner upon reaching the back of the swarm than reaching the front. We made this difference in thresholds so that stalker bees can lead the bees in the front for longer. The bees in the front are the most confused bees (see simulation results in Figures 8 and 9), as they can see no other bees in front, and when they look back and try to align with the bees behind, they would end up looking forward again, with no bees to follow. On the contrary, the bees in the back can see forward and follow the bees in front, hence the less strict the turning threshold of the stalker bees is in this case.

In real bee swarms, when a stalker bee returns to the back, it flies along the edge and near the bottom of the swarm so that it affects the other bees less. We consider this fact in our model, by making a returning stalker bee less visible to the rest. More specifically, when a stalker bee, bee s , flies to the back of the swarm, that is, in the wrong direction, we reduce by 10 times the values of the vision coefficients w_{js} , for all other bees j , as computed from (7). In other words, stalker bees flying forward are 10 times more visible to the rest of the bees than when flying backward.

3 Numerical results

We consider a two dimensional *horizontal* swarm of size $N = 630$, where $N_s = 30$ are stalker bees and $N_f = 600$ are followers (note that stalkers are less than 5% of the total population). All stalkers fly in the positive x -direction, which is the direction of the target. The equations of motion (1) and (5)/(6) are discretized using the 4th order Runge-Kutta method.

The follower bees' initial positions are randomly generated in a rectangular box of 15×10 . Their velocities are also randomly initialized with both the x -component and the y -component between -1 and 1. The leader bees' positions are randomly initialized in a smaller rectangular box (size 10×6) centred around $(7.5, 5)$. For a better mixing, we initialize half of the stalkers to start off flying in the desired direction, while the other half start moving in the opposite way. In Model I the stalkers's initial velocities have a magnitude of 0.1.

We designed various numerical experiments for the bee swarm model (1) and (5)/(6) in order to address some of the issues studied in experiments: angle distributions and directionality, efficiency of flight guidance, speed of swarm versus speed of stalkers. Unless otherwise noted, in all simulations, the following parameters are fixed: interaction strengths and ranges, except alignment strength: $C_a = 0.5$, $C_r = 2$, $l_a = 5$, $l_r = 1.5$, $l_{al} = 2.5$; blind zone coefficients: $a = 3$, $b = 1.5$, $d = 5$, alignment function: $h = 7$, $s = 0.7$. The cone of vision considered here is a little smaller than the bee's field of view observed in experiments [28, 29]. This is compensated however by the extra feature we have incorporated in the model, which assigns full cone of vision to bees flying below a certain threshold.

Efficiency of flight guidance: Model I or Model II? First we investigate which of the two models for the flight of the stalker bees ((5) or (6)) is more efficient. For this purpose we design the following numerical experiment. Consider Model I with the horizontal acceleration \mathbf{a}_0 of the stalker bees having either magnitude 0.62 (when leader bees streak forward) or 0.1 (when leader bees return to the rear). We run the model up to $T = 800$ and calculate the average velocities of the stalker bees when they fly forward and backward, respectively. As an example, for $C_{al} = 0.1$, we find the forward and backward-flying average velocities of the stalker bees to be 2.47 and -0.94 , respectively. Next, we run Model II for the same values of the parameters, and take the horizontal velocity \mathbf{v}_0 of the stalker bees to be either the forward or backward average velocities of Model I, according to the direction of travel. Hence, stalker bees in the two models fly at the same average velocities in both directions.

We performed the experiment described above and compared the efficiency of the flight guidance, that is, the amount traveled by the swarm in the direction of the target or equivalently, the speed of the swarm in the desired direction of travel. We considered various values of the alignment coefficient: $C_{al} = 0.1, 0.2, 0.35$ and 0.5 . In all runs we observed that the flight guidance in Model I is more efficient than in Model II. Table 1 shows the distance traveled in the positive x direction (direction of travel) for the two models, as well as the efficiency gain of Model I over Model II. Note that Model I becomes significantly more advantageous for larger C_{al} . The explanation lies in the fact that in Model II the stalkers' return flight is performed at a uniform speed that is relatively larger compared to the speed of the uninformed bees, thus generating confusion and leading them in the wrong direction. In contrast, in Model I, returning bees accelerate steadily after turning direction, and fly at relatively low speeds for the first segment of the returning flight, when they are still in front of the swarm and in the cone of vision of most bees. The results presented in Table 1 have been confirmed with several other random initial conditions. We also tested several cases

	Model I	Model II	Efficiency gain
$C_{al} = 0.1$	67.56	61.93	9.09 %
$C_{al} = 0.2$	106.15	97.58	8.78 %
$C_{al} = 0.35$	141.16	122.01	15.69 %
$C_{al} = 0.5$	166.34	122.11	36.22%

Table 1: Efficiency of flight guidance in the two models: distance travelled in the direction of the target (shown in columns 2 and 3) for various values of the alignment strength C_{al} . The experiment has been designed so that the stalker bees fly at the same forward and backward average velocities in both models. Model I is more efficient, in particular for larger C_{al} , as illustrated in the last column. The results are based on a single, typical simulation, using random initial conditions.

where we made the returning stalkers completely invisible to the rest, and again, we found Model I to be preferable to Model II.

Time evolution of the swarm, flight angle distribution. In the rest of the paper we focus our attention on Model I, the more advantageous of the two models.

Figure 4(a) illustrates the evolution of the x -coordinate of the centre of mass of the swarm, after the initialization phase has passed ($t \geq 200$), for various values of the alignment strength C_{al} . Note that for each value of C_{al} the swarm reaches quasi steady state motions, where the centre of mass travels at constant speeds (the slopes of the graphs) in the desired direction.

In Figure 4(b) we plot the trajectories of the centre of mass, along with the highest and the lowest¹ bee locations in the swarm, from $t = 0$ to $t = 800$, for the values of C_{al} used in Table 1 and Figure 4(a). The plot shows that after an initialization phase, during which the swarm expands, the bees remain confined within a horizontal band of height ≈ 21.5 . During flight, the bees redistribute their locations within the swarm, however the swarm translates as a whole in the desired direction. Snapshots of the swarm at various times (see Figures 8 and 9) show that the swarm reaches a circular shape which it maintains for long times. Qualitatively similar graphs were obtained for various other initial conditions that we tested.

We point out that the efficiency of flight guidance is essentially affected by the size of the cone of vision. An experiment using a wider field of vision with $a = 5$, $b = 2$ (see Figure 3) showed that this increase in visibility almost doubled the distance travelled by the swarm. For instance, with $C_{al} = 0.2$, the values of a and b set originally (and used in all experiments presented in the paper) result in a distance of 106.15 (column 2, Table 1), while the latter choice yields a distance of 207.97! Similar results were found using other values for a , b , and C_{al} . This outcome is very much expected: larger fields of vision for follower bees means that they see the stalkers more often and a better guidance is achieved. However, a too aligned swarm may not be realistic, and this aspect will be addressed shortly. When results for two blind zones are compared though, there is a caveat that has to be mentioned: a wider field of vision makes the vision indicators $\sum_{j \neq i} w_{ij}$ larger. In the model, when their vision indicators drop below certain thresholds, stalker bees decide to turn and follower bees get assigned random velocities. Therefore, these thresholds have to be adjusted manually when a different field of vision is considered. Regardless of this issue though, it is clear

¹The swarm considered in this paper is *horizontal*, hence phrases such as “the highest and lowest locations” or “swarm height” refer to the horizontal y -variable, not to the vertical direction.

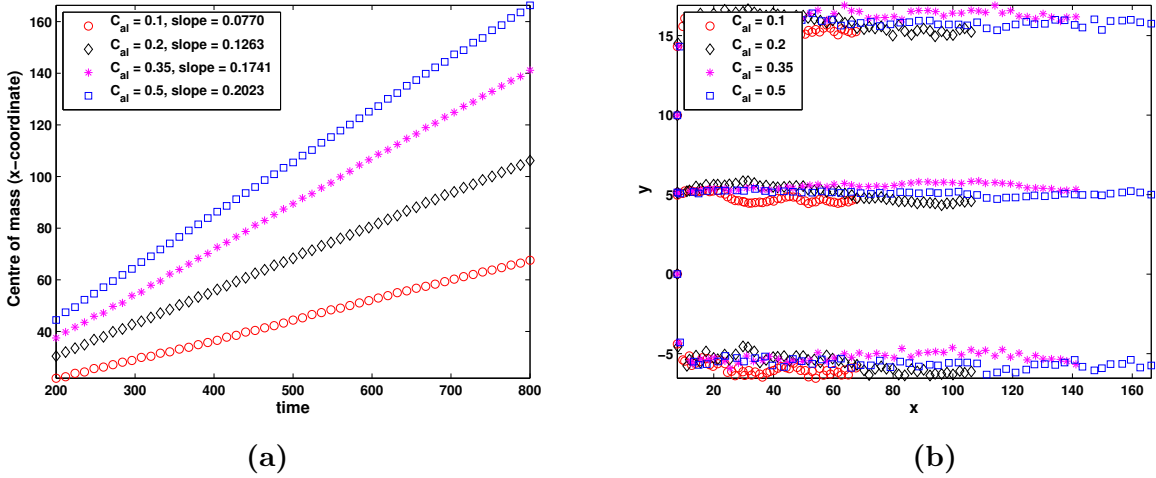


Figure 4: (a) Time evolution of the x -coordinate of the centre of mass. The slopes yield the average velocities of the swarm. (b) Trajectories of the centre of mass, along with the highest and the lowest bee locations in the swarm. The plot shows the confinement of the swarm within a horizontal band of height ≈ 21.5 .

from the various experiments we performed that increasing the field of vision always improves, and sometimes dramatically, the flight efficiency.

The distribution of flight angles in bee swarms has been observed experimentally — see the photographic study in [13] and the video data processing from [15]. Both these studies show a fairly wide distribution of flight angles that is peaked at the desired direction of flight. In particular, the video recordings from [15] show a generally chaotic swarm, with bees flying in all directions and with a wide range of speeds.

We test Model I for various values of the alignment strength C_{al} and compare the angle distribution with the experimental observations. In Figure 5 we plot the mean and the variance of the flight angles of the bees as a function of time, for various values of C_{al} . As expected, the higher the alignment strength, the more organized and aligned the flight of the swarm: the mean angle fluctuates less around the desired direction of travel $\theta = 0$ (Figure 5(a)) and the variance reduces significantly (Figure 5(b)).

For a better visualization of the swarm states and their evolution, we selected several instances of time (initial time and times of highest, lowest and intermediate variance values) and plotted the histogram of the flight angles at these times, along with the snapshots of the entire swarm. See Figures 6, 8 for plots corresponding to $C_{al} = 0.1$ and Figures 7, 9 for plots corresponding to $C_{al} = 0.5$. The range of flight angle is $[-\pi, \pi]$. Note in Figures 6 and 8 that even at time instances when the variance is low ($t = 600$), the swarm flight is fairly chaotic. The alignment of uninformed bees with the leaders is mainly local and the more distant bees seem to fly in a random fashion. In contrast, Figures 7 and 9 which correspond to $C_{al} = 0.5$, show a large degree of alignment. At $t = 454$, where the variance is the lowest, the swarm seems too aligned to be realistic. Even at times where the variance takes intermediate values ($t = 490$) the alignment seems too strong. From this respect, Figures 6 and 8 (for $C_{al} = 0.1$) seem to match better the experimental data, where

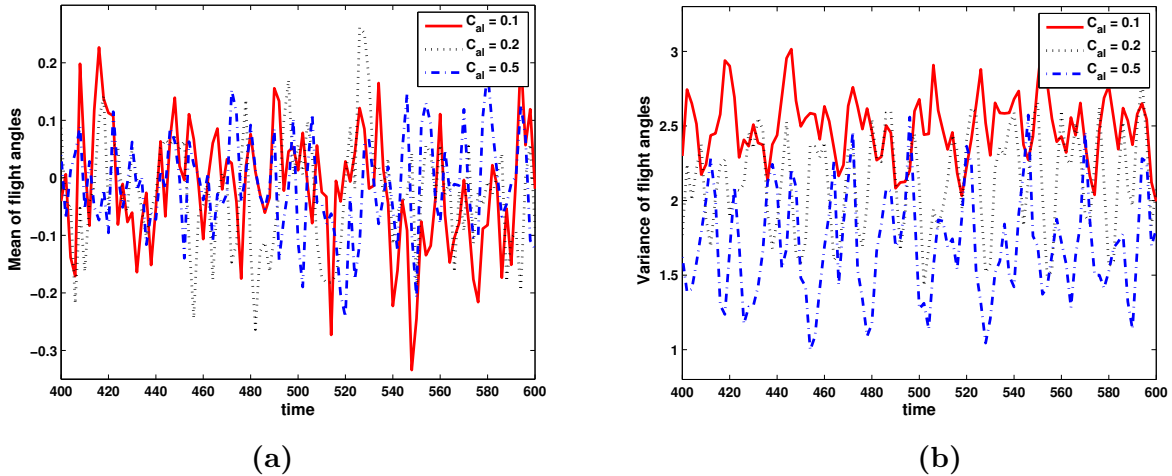


Figure 5: Time evolution of (a) mean of flight angles and (b) variance of flight angles. Note that smaller values of the alignment strength C_{al} corresponds to higher variance (higher disorder in the swarm), as bees are less prone to align.

bees in swarms have been observed to fly in all directions.

Advantages of returning faster/slower to the rear. We constructed an experiment to test the optimal returning acceleration of starker bees given a particular alignment strength and constant forward acceleration. We set the forward acceleration to 0.62 and $C_{al} = 0.2$.

The results are summarized in Table 2. Taking as reference the run with returning acceleration $\mathbf{a}_0 = -0.1\mathbf{i}$ (\mathbf{i} is the unit vector in the positive x direction), we observe the following. A faster returning acceleration ($\mathbf{a}_0 = -0.2\mathbf{i}, -0.3\mathbf{i}$) results in a faster return, which in turn results in more streaks through the swarm. On the other hand, faster returning streakers create more confusion, as uninformed bees will tend to align with their wrong direction of flight. The overall effect of having more frequent streaks but increased confusion, in this experiment, is an improvement of the efficiency of the flight — see last column of Table 2. However, higher values of \mathbf{a}_0 (comparable to the forward acceleration) would slow down the swarm (results not shown here).

Decreasing the returning acceleration results in a mix of gain/loss of efficiency, as noted from the last column of Table 2. We presented results up to $\mathbf{a}_0 = -0.005\mathbf{i}$, as beyond this value the flight efficiency drops sharply. We point out that lower acceleration may result in significant efficiency gains ($\mathbf{a}_0 = -0.03\mathbf{i}$ for instance corresponds to an efficiency gain of more than 8%). These results have to be interpreted in connection with the hypothesis that we made regarding the reduced visibility of a returning starker bee. We made a returning starker bee 10 times less visible to the rest of the swarm than it would be if it flew forward. This assumption was made to model the deliberate flight of the returning streakers along the edges and near the bottom of the swarm in order to minimize its interference with the motion of the swarm in the desired direction. Our *nonlinear* model selects a few values of the returning acceleration which yield local maxima for the flight efficiency, hence capturing the delicate balance between faster returns (and more streaks) and the increased confusion they create, a balance which evolution and adaptation must have sorted out.

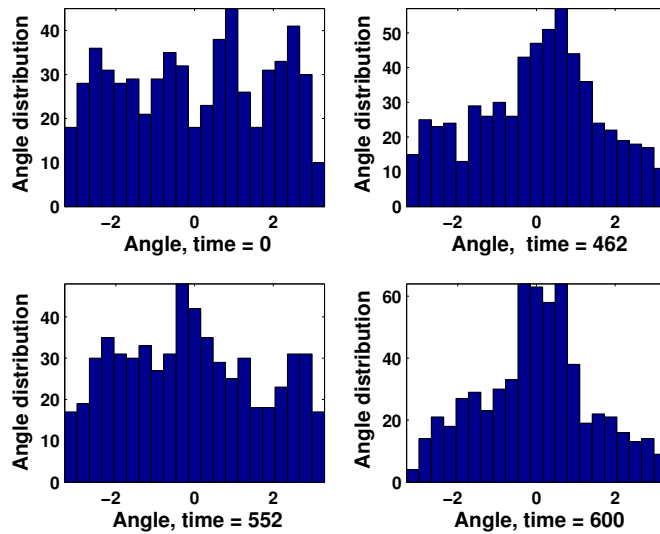


Figure 6: Distribution of flight angles at various times ($C_{al} = 0.1$). At $t = 0$ the distribution of flight angles is very even, as uninformed bees have random orientations. Times $t = 462, 552$, and 600 correspond to instances where the variance of flight angles has an intermediate, the highest and the lowest values, respectively (see Figure 5(b)). Snapshots of the swarm at these time instances are plotted in Figure 8.

Efficiency in terms of the number of stalker bees. One of the most interesting aspects of this model is its robust flight efficiency as the number of stalker bees are being decreased. The previous numerical experiments concern a swarm of size $N = 630$ with $N_s = 30$ followers (less than 5%, as suggested by observations). We now consider a swarm of the same size, but with $N_s = 24, 18, 12, 6$, respectively. As initial data we take the random initial conditions of the run discussed in the previous paragraphs, except that now, a smaller component of the bees evolve according to (5).

The results are summarized in Table 3. The entries in the table represents the distance travelled by the swarm in the direction of the target, along with the gain/loss of efficiency as compared to the reference run $N_s = 30$. We considered various values of the alignment strengths, $C_{al} = 0.1, 0.2, 0.35, 0.5$. In fact, the second column in the table, corresponding to $N_s = 30$ is the same as the second column in Table 1. The (perhaps surprising) result is that decreasing the number of stalker bees may increase the efficiency of the flight, and when it affects it negatively, it does so by a relatively small amount. Also, reasonably good efficiency is achieved with as low as $N_s = 6$ stalker bees (less than 1% of the size of the swarm)! Efficiency drops sharply however if we use just a single stalker. A similar feature has been observed in the model of Couzin *et. al* [14] that supports the “subtle guide” hypothesis of scout bee guidance. More specifically, it is noted in [14] that for a given accuracy, the larger the group is, the smaller the proportion of the informed individuals is needed to guide the group with that accuracy. In [14], the maximum size of a swarm is $N = 200$ and in such swarms 3% of informed individuals would do almost as good guidance as 25%. Our observations, as well as theirs, suggest that, as far as flight guidance is concerned, bee swarms would achieve little benefit from having larger scout populations. However, this statement

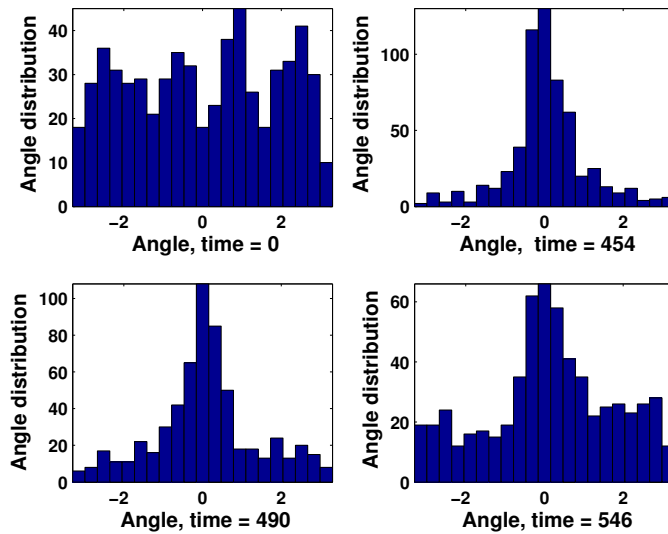


Figure 7: Distribution of flight angles at various times ($C_{al} = 0.5$). Times $t = 454, 490$, and 546 correspond to instances where the variance of flight angles has the lowest, an intermediate, and the highest values, respectively (see Figure 5(b)). Snapshots of the swarm at these time instances are plotted in Figure 9.

has to be taken with care, as observations in [30] indicate that a reasonable number of participants are needed in the pre-flight task of choosing a nest site.

Swarm split. There are rare occurrences in nature where the scout bees fail to agree on a single new nest location. When this happens, the swarm takes off with approximately half of the scout bees streaking in the direction of nest A and the other half streaking in the direction of nest B. This causes confusion among the followers and results in a split and/or loss of the queen bee. In our model, we experimented with breaking up the scout bees. Two different results were obtained when using different initial conditions. The entire swarm either follows one single group of leaders or stops moving. Split of the swarm was not obtained. In the experiment we made half of the stalker bees streak in the x-direction and other other half streak in the y-direction. The swarm starts off moving diagonally (in both the x-direction and the y-direction), trying to follow both groups of stalker bees. This causes the stalker bees to move towards the edge of the swarm, thus resulting in less alignment force being acted on the overall swarm. In the extreme case where both groups of leader bees are at the very edge, the swarm moves so slowly that it reaches a "quasi-steady" state. In the other case, one group of streak bees dominates and the other group of stalker bees is lost.

4 Discussion

Studies involving photographic analysis [13] and video data processing [15] revealed various characteristics of the flying swarms. The swarms studied in [13] (also reviewed in Chapter 8 of [11]) traveled a distance of 270 m to a bait hive in a very similar fashion: immediately after take off,

	Average return speed	Distance travelled	Efficiency gain
$\mathbf{a}_0 = -0.005$	-0.18	92.13	-13.20%
$\mathbf{a}_0 = -0.02$	-0.37	104.26	-1.78%
$\mathbf{a}_0 = -0.03$	-0.47	115.10	8.43%
$\mathbf{a}_0 = -0.04$	-0.55	106.25	0.09%
$\mathbf{a}_0 = -0.05$	-0.63	102.18	-3.74%
$\mathbf{a}_0 = -0.1$	-0.89	106.15	0%
$\mathbf{a}_0 = -0.2$	-1.30	109.91	3.54%
$\mathbf{a}_0 = -0.3$	-1.61	111.46	5.00%

Table 2: Efficiency of returning acceleration: average returning velocity of the starker bees and total distance travelled by the entire swarm (shown in columns 2 and 3) for various values of the returning acceleration \mathbf{a}_0 of starker bees. The experiment has been designed so that the alignment strength stays constant in these runs ($C_{al} = 0.2$). Efficiency is calculated based on total distance travelled in the direction of target using $\mathbf{a}_0 = -0.1 \mathbf{i}$ as reference.

	$N_s = 30$	$N_s = 24$	$N_s = 18$	$N_s = 12$	$N_s = 6$
$C_{al} = 0.1$	67.56	67.62 (+0.08%)	69.75 (+3.24%)	69.51 (+2.88%)	63.45 (-6.08%)
$C_{al} = 0.2$	106.15	106.46 (+0.29%)	101.55 (-4.33%)	102.33 (-3.59%)	96.40 (-9.18%)
$C_{al} = 0.35$	141.16	140.47 (-0.48%)	137.94 (-2.28%)	140.32 (-0.59%)	125.81 (-10.87%)
$C_{al} = 0.5$	166.34	159.33 (-4.21%)	163.07 (-1.96%)	159.96 (-3.83%)	144.48 (-13.14%)

Table 3: Efficiency of flight guidance as the number N_s of informed individuals decreases. The entries in the table represent the distance traveled in the desired direction and in parentheses is the gain/loss of efficiency as compared to the reference run $N_s = 30$. Lower proportions of starker bees do comparable (in some cases better) guidance to the swarm. Even $N_s = 6$ starker bees (less than 1% of the size of the swarm) can achieve reasonably good efficiency.

there was an initial stage of very slow motion, followed by a steady acceleration for the first 90 m. At that point, the swarms have reached peak flight speeds of 6-7 km/h, which they maintained until they came within 30-50 m from the new nest. During the final 30 m, the swarm moved slowly and eventually came to a halt. The photos showed that most bees flew slowly, in curved and loopy paths, while a small percentage of the bees streaked through the swarm, in straight and level flights toward the destination, at the maximum speed of a worker bee, which is 34 km/h.

Our model yields solutions that are qualitatively consistent with the swarm flight and description above. First, it recovers the slowly accelerating motion on the initial flight segment, when the swarm organizes itself from a a very chaotic state to a fairly organized flight. Second, the swarms in the model reach constant travel speeds, as the real bee swarms do, which they can maintain for very long times. The individual trajectories of the follower bees are loopy and lack a definite sense of direction, but the swarm as a group moves consistently in the direction of the target. Depending on the strength of alignment, the model yields different ratios between the average speed of a stalker and the achieved average speed of the swarm. For instance (see Figure 4(a)), corresponding to $C_{al} = 0.5$ we have an average swarm velocity of 0.2023, which is about 8.3% of the average velocity 2.4290 of the stalker bees. This is consistent with observations, as bee swarms fly at average velocities of 3 km/h, which is about 8.8% of the maximum speed 34 km/h of a stalker bee.

Social interactions among bees are very difficult to quantify and we are not aware of any experimental data that would indicate a particular potential as a suitable model for such interactions. We chose the Morse potential (for reasons indicated in Section 2) to model attraction and repulsion, and we made suitable choices for the interaction parameters C_a, C_r, l_a , and l_r in order to obtain aggregations in circular/elliptical clumps, the appropriate geometrical shape for bee swarms. As shown in [21], dynamics using Morse potential can give rise to various other aggregation patterns, such as rings, ring clumps, annular groups, etc. Several other interaction potentials have been used in the aggregation literature, in particular power-law potentials [23]. Given the very diverse range of aggregation patterns that can be obtained with such potentials, it is very likely that other choices of the potential would produce results similar to those presented in the present research. This investigation however was outside the scope of the paper.

It was shown in [13] that the distribution of flight angles becomes more clustered around the travel direction as the flight progresses. This means that during the flight, the bees increasingly adopted flight directions that were aligned with the direction of the new nest, suggesting a chain reaction and a spread of information (regarding the desired direction of flight) among the bees. The more recent studies from [15] confirm these results, but also suggest that the distribution of the flight angles is wider than initially thought (meaning less directed and more random flights).

In light of these experimental observations, we designed a numerical experiment, where the strength of the alignment coefficient gradually increases as time progresses. One can motivate the increase in C_{al} by bees acquiring a better sense of the correct travel direction, due to the spread of information mentioned above. Starting at $C_{al} = 0.05$, we increase the alignment strength by 0.05 at every 100 time units and run it to $t = 800$ — see Figure 10. We observe indeed an increase in the average velocity of the swarm and hence in the efficiency of the flight guidance, as noted by observations. Equivalently, the increase of C_{al} induces a tighter and more clustered distribution of flight angles (see Figures 6 and 7, as well as the swarm snapshots from Figures 8 and 9), a feature also consistent with observations.

A question which is unanswered yet [11] is how a bee swarm comes to a halt when it arrives within 100 meters of its new nest. A previous model [16] achieved the braking by a gradual removal

of the scouts. Our model works so efficiently with very small numbers of streakers, that gradual removal of scouts does not brake the swarm significantly (this was discussed above in a paragraph of Section 3 — see Table 3). Only when all (or a very high portion of) scouts stop streaking, the swarm in our model comes indeed to a complete stop. We point out again that this feature contrasts with a previous model for streaker bee flight guidance [16], which is much more sensitive to the number of scouts in the swarm.

Our model is different from a previous model considered in the literature [16, 17], as it evolves continuously in time according to Newton’s law of motion, as opposed to having prescribed discrete-time interaction rules. The models do have however clear similarities. For instance, in both models, attractive and repulsive interactions with neighbours are based on a metric (as opposed to topological) distance; in our model the interaction zones are set by the Morse potential, in theirs, they are set explicitly. Also, in both models, a reference individual aligns only with neighbours that fly at least *two times* faster (alignment in [17] however uses a topological metric). Finally, although the formulation of our model is continuous, simulations use discrete approximations, and in that sense our model is not so far removed from the inherently discrete models of [16, 17]. In addition to previous models, we do consider a cone of vision/ blind zone for the individuals, as well as various other realistic features regarding the bees on the edges of the swarm.

To conclude, our model captures the essential features of flights of bee swarms to new nests, when streaking is considered as the underlying guidance mechanism provided by the scouts. The swarms in our model have qualitative features that closely match real swarms in terms of average swarm speed, flight angle distribution, individual trajectories of the follower bes, etc. An extension of this model to 3 dimensions can be easily done conceptually, but it will introduce some difficulties in its numerical implementation. We plan to address this extension in future work.

References

- [1] T. Pitcher, A. Magurran, I. Winfield, Fish in larger shoals find food faster, *Behav. Ecol. and Sociobiology* 10 (1982) 149151.
- [2] S. Camazine, J.-L. Deneubourg, N. R. Franks, J. Sneyd, G. Theraulaz, E. Bonabeau, *Self-organization in biological systems*, Princeton Studies in Complexity, Princeton University Press, Princeton, NJ, 2003, reprint of the 2001 original.
- [3] W. D. Hamilton, Geometry for the selfish herd, *J. Theor. Biol.* 31 (1971) 295–311.
- [4] J. Krause, G. D. Ruxton, *Living in groups*, Oxford University Press, Oxford, UK, 2002.
- [5] A. Okubo, D. Grünbaum, L. Edelstein-Keshet, The dynamics of animal grouping, in: Okubo A., Levin S., *Diffusion and ecological problems: modern perspectives*, Springer, N.Y., 2001, pp. 197–237.
- [6] T. Seeley, R. Morse, P. Visscher, The natural history of the flight of honey bee swarms, *Psyche* 86 (1979) 103–113.
- [7] P. Berthold, U. Querner, Genetic basis of migratory behavior in European warblers, *Science* 212 (1981) 77–79.

- [8] J. J. Dodson, The nature and role of learning in the orientation and migratory behavior of fishes, *Environmental Biology of Fishes* 23 (3) (1988) 161–182.
- [9] M. L. Winston, *The Biology of the Honey Bee*, Harvard University Press, Cambridge, MA, 1987.
- [10] M. Lindauer, Schwarmbiene auf Wohnungssuche, *Zeitschrift für Vergleichende Physiologie* 37 (1955) 263–324.
- [11] T. D. Seeley, *Honeybee Democracy*, Princeton University Press, Princeton, NJ, 2010.
- [12] A. Avitabile, R. A. Morse, R. Boch, Swarming honey bees guided by pheromones, *Annals of the Entomological Society of America* 68 (1975) 1079–1082.
- [13] M. Beekman, R. L. Fathke, T. D. Seeley, How does an informed minority of scouts guide a honeybee swarm as it flies to its new home?, *Animal Behaviour* 71 (2006) 161–171.
- [14] I. D. Couzin, J. Krause, N. R. Franks, S. A. Levin, Effective leadership and decision making in animal groups on the move, *Nature* 433 (2005) 513–516.
- [15] K. Schultz, K. Passino, T. Seeley, The mechanism of flight guidance in honeybee swarms: subtle guides or stalker bees?, *Journal of Experimental Biology* 211 (2008) 3287–3295.
- [16] S. Janson, M. Middendorf, M. Beekman, Honey bee swarms: How do scouts guide a swarm of uninformed bees?, *Animal Behaviour* 70 (2005) 349–358.
- [17] K. Diwold, T. M. Schaerf, M. R. Myerscough, M. Middendorf, M. Beekman, Deciding on the wing: in-flight decision making and search space sampling in the red dwarf honeybee *Apis florea*, *Swarm Intell.* 5 (2011) 121–141.
- [18] T. Latty, M. Duncan, M. Beekman, High bee traffic disrupts transfer of directional information in flying honey bee swarms, *Animal Behaviour* 78 (2009) 117–121.
- [19] M. Ballerini, N. Cabibbo, R. Candelier, A. Cavagna, E. Cisbani, I. Giardina, V. Lecomte, A. Orlandi, G. Parisi, A. Procaccini, M. Viale, V. Zdravkovic, Interaction ruling animal collective behaviour depends on topological rather than metric distance: evidence from a field study, *Proc. Natl. Acad. Sci.* 105 (2008) 1232–1237.
- [20] H. Levine, W.-J. Rappel, I. Cohen, Self-organization in systems of self-propelled particles, *Phys. Rev. E* 63 (1) (2000) 017101.
- [21] M. R. D’Orsogna, Y.-L. Chuang, A. L. Bertozzi, L. S. Chayes, Self-propelled particles with soft-core interactions: patterns, stability and collapse, *Phys. Rev. Lett.* 96 (10) (2006) 104302.
- [22] R. Lukeman, Y.-X. Li, L. Edelstein-Keshet, A conceptual model for milling formations in biological aggregates, *Bull. Math. Biol.* 71 (2) (2009) 352–382.
- [23] T. Kolokolnikov, H. Sun, D. Uminsky, A. L. Bertozzi, A theory of complex patterns arising from 2D particle interactions, *Phys. Rev. E, Rapid Communications* 84 (2011) 015203(R).
- [24] A. Mogilner, L. Edelstein-Keshet, L. Bent, A. Spiros, Mutual interactions, potentials, and individual distance in a social aggregation, *J. Math. Biol.* 47 (2003) 353–389.

- [25] D. D. Holm, V. Putkaradze, Aggregation of finite-size particles with variable mobility, *Phys Rev Lett.* 95:226106.
- [26] N. E. Leonard, E. Fiorelli, Virtual leaders, artificial potentials and coordinated control of groups, *Proc. of the 40th IEEE Conference on Decision and Control* (2001) 2968–2973.
- [27] F. Cucker, S. Smale, Emergent behavior in flocks, *IEEE Trans. Automat. Control* 52 (5) (2007) 852–862.
- [28] R. Seidl, W. Kaiser, Visual field size, binocular domain and the ommatidial array of the compound eyes in worker honey bees, *J. Comp. Physiol. A* 143 (1981) 17–26.
- [29] W. Stürzl, N. Boeddeker, L. Dittmar, M. Egelhaaf, Mimicking honeybee eyes with a 280° field of view catadioptric imaging system, *Bioinsp. Biomim.* 5 (2010) 036002.
- [30] J. Makinson, B. Oldroyd, T. Schaerf, W. Wattanachaiyingchareon, M. Beekman, Moving home: nest-site selection in the Red Dwarf honeybee (*Apis florea*), *Behav. Ecol. Sociobiol.* 65 (5) (2011) 945–958.

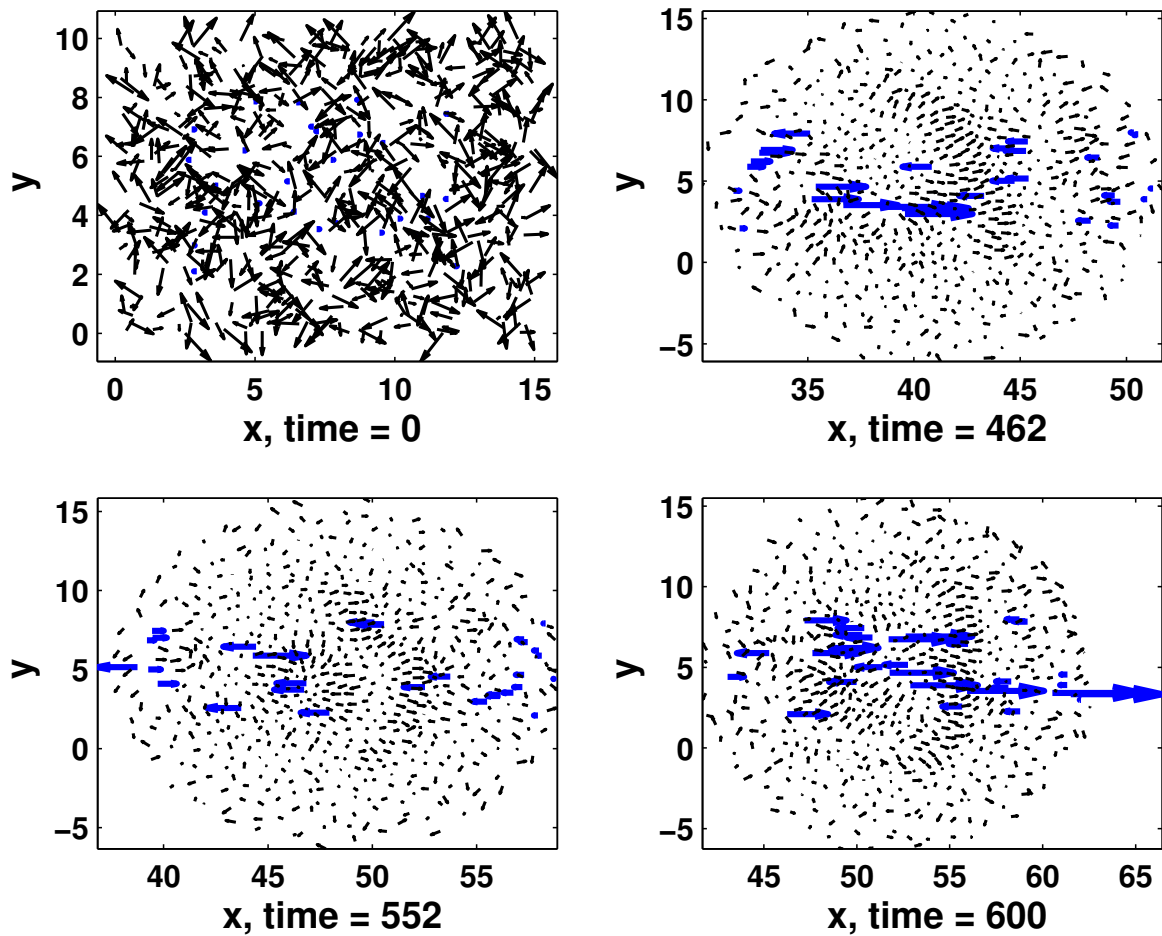


Figure 8: Snapshots of the swarm at various times ($C_{al} = 0.1$): $t = 0, 462, 552,$ and 600 . The latter three times correspond to instances where the variance of flight angles has an intermediate, the highest and the lowest values, respectively (see Figures 5(b) and 6). The leader bees are represented by thick arrows and follower bees by thin arrows.

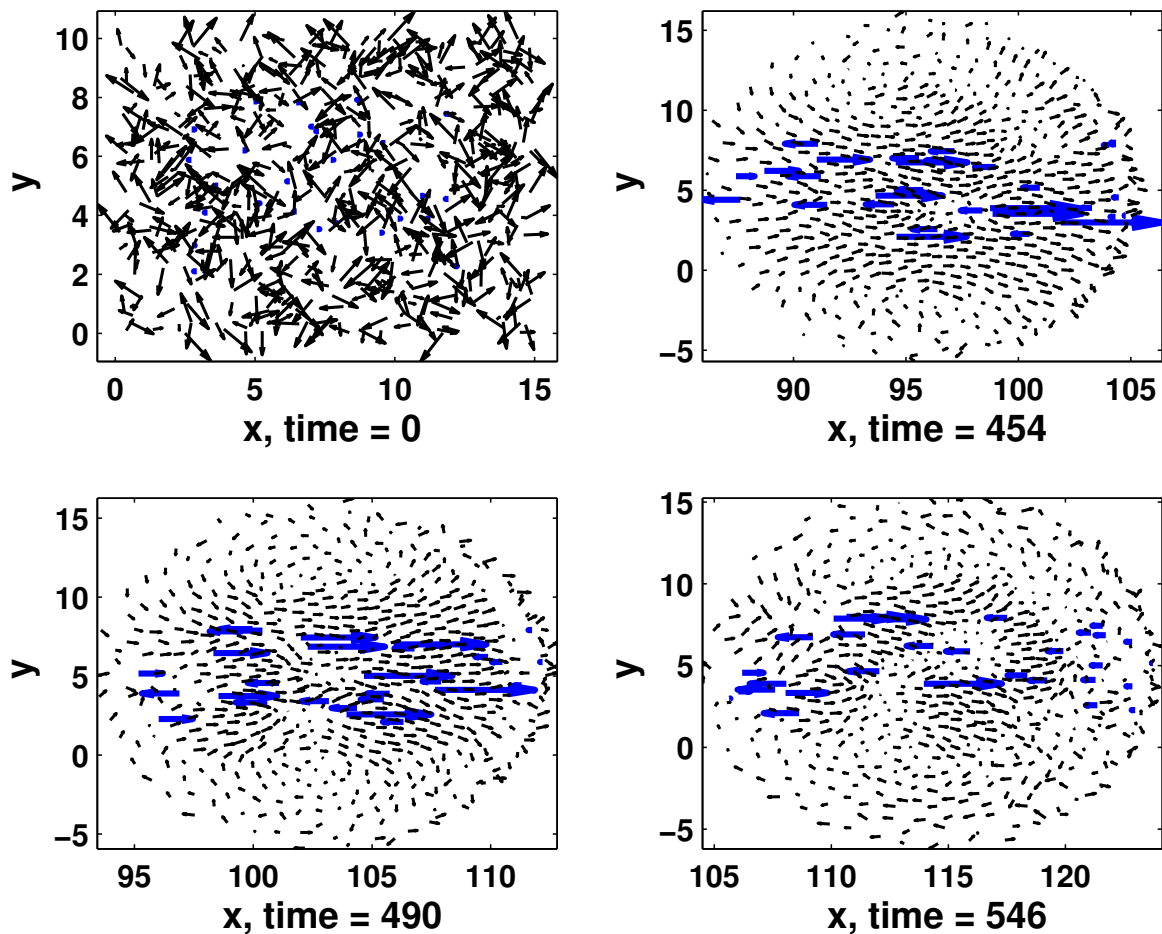


Figure 9: Snapshots of the swarm at various times ($C_{al} = 0.5$): $t = 0, 454, 490$, and 546 . The latter three times correspond to instances where the variance of flight angles has the lowest, an intermediate, and the highest values, respectively (see Figures 5(b) and 7). The leader bees are represented by thick arrows and follower bees by thin arrows.

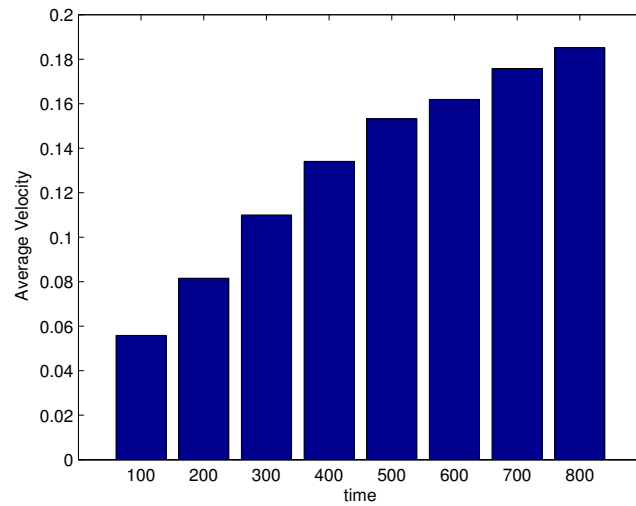


Figure 10: Gradual increase of the alignment strength C_{al} increases the average velocity of the swarm. Starting at $C_{al} = 0.05$, the alignment strength is increased by 0.05 at every 100 time units, so in the last time segment $C_{al} = 0.4$. This feature was implemented to mimic the steady acceleration of a real bee swarm, due to a chain reaction and spread of information among the uninformed bees. Here, the learning process is modelled by an increasing C_{al} (through the flight, followers learn to align themselves better).